Research Article

Jinping Luo, Guoxiang Huang, Yanni Shao, Jian Liu*, and Quanyi Xie

Laboratory test and numerical simulation of composite geomembrane leakage in plain reservoir

https://doi.org/10.1515/geo-2020-0247
received August 01, 2019; accepted March 29, 2021

Abstract: Plain reservoir plays an important role in alleviating water shortage in plain areas which are generally crowded with large populations. As an effective and cheap anti-seepage measure, geomembrane is widely applied in plain reservoirs. Therefore, it is necessary to investigate the seepage discharge caused by composite geomembrane leakage. The laboratory test and numerical calculation are carried out in this paper to analyze the influence of three factors (i.e., water head, leakage size, and leakage location) on seepage discharge. It is found from the results of the orthogonal and single-factor analysis that the impact order of the three factors on the seepage discharge of plain reservoir is: distance from dam toe > water head > leakage size. Moreover, the seepage discharge increases as the water head, leakage size, and leakage quantity increase, in a linear relation. The opposite trend can be sawed in the seepage discharge when the distance from dam toe rises. Furthermore, a threshold distance is innovatively presented based on the results of numerical analysis. The ranking of three factors has enlightening significance for future scholars to track and study key issues of the leakage of composite geomembrane. The threshold distance presented in this paper is beneficial for engineers to manage and maintain the reservoir. Generally, the findings of this study can be beneficial to deepen the understanding of the influence of composite geomembrane leakage on the plain reservoirs.

Keywords: composite geomembrane, leakage, plain reservoir, numerical simulation

*** Corresponding author: Jian Liu,** School of Qilu Transportation, Shandong University, No. 17922, Jingshi Road, Jinan 250061, China, e-mail: liujianshanda@163.com, tel: +86-152-6917-9376
Jinping Luo: Academy of New Energy Engineering, PowerChina Huadong Engineering Corporation Limited, No. 201, Gaojiao Road, Hangzhou 310000, China, e-mail: luo_jp@ecidi.com
Guoxiang Huang: School of Civil Engineering, Shandong University, No. 17922, Jingshi Road, Jinan 250061, China, e-mail: 201914602@mail.sdu.edu.cn
Yanni Shao: School of Civil Engineering, Shandong University, No. 17922, Jingshi Road, Jinan 250061, China, e-mail: yannishaosdu@163.com
Quanyi Xie: School of Civil Engineering, Shandong University, No. 17922, Jingshi Road, Jinan 250061, China, e-mail: quanyixiesdu@163.com

1 Introduction

The plain reservoir is an important engineering measure to solve the drought and water shortage in the plain area, which is widely distributed in the central and eastern plains of China [1–3]. In recent years, with the construction of the South-to-North Water Transfer Project, a large number of plain reservoirs, open channels, tunnels, and other supporting water storage and diversion projects were built in China [4,5]. Leakage is common in all kinds of infrastructure projects, which is easy to cause serious disasters. Many researchers have studied the leakage of infrastructure. Some researchers have studied the seepage impact on the interface behavior of tunnel [6–8]. Peng and Wang [9] and Zhao et al. [10] studied the inductive factors and nondestructive detection methods of earth dam leakage. The seepage and scour mechanism of the contact surface between culvert pipe and dam body has also been studied by some researchers [11,12].

Plain reservoirs are generally built in the densely populated plain area; once leakage disaster occurs, it will bring great disaster to the safety of social life and property. Composite geomembrane is used in most plain reservoirs to prevent water leakage [13–16]. Although the composite geomembrane has some advantages of good antibody performance, strong extensibility, and simple construction, it is prone to small damage in the construction process [17–19] (shown in Figure 1). Barroso [20] investigated more than 3.25×10^6 m^2 composite geomembranes, and the results showed that the leakage of the size of 0.5–20 cm accounts for 85.8%.

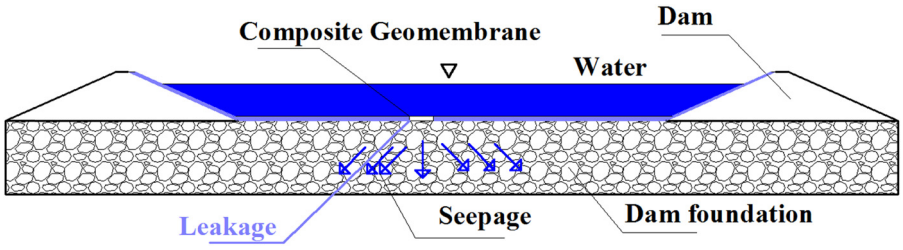

Figure 1: Realistic reflection of the designed tests.

In recent years, many studies have researched the leakage of composite geomembrane [21–25]. Giroud et al. [26] proposed that the underlying layer should play an auxiliary anti-seepage role and form an impermeable layer together with the geomembrane, and through a large number of studies, a simplified semiempirical formula for calculating the seepage of leakage in good contact and bad contact between geomembrane and underlay was presented. Wu and Yu [27], Liu et al. [28], and Li [29] qualitatively analyzed the influence of leakage of composite geomembrane on seepage discharge of earth-rock dam through the indoor model test. These studies found that the seepage discharge increases with the increase of leakage size and leakage diameter ratio. Sun et al. [30] and Cen et al. [31] established the numerical model of the leakage zone of composite geomembrane and analyzed the influence of the composite geomembrane leakage on the seepage field of the leakage part.

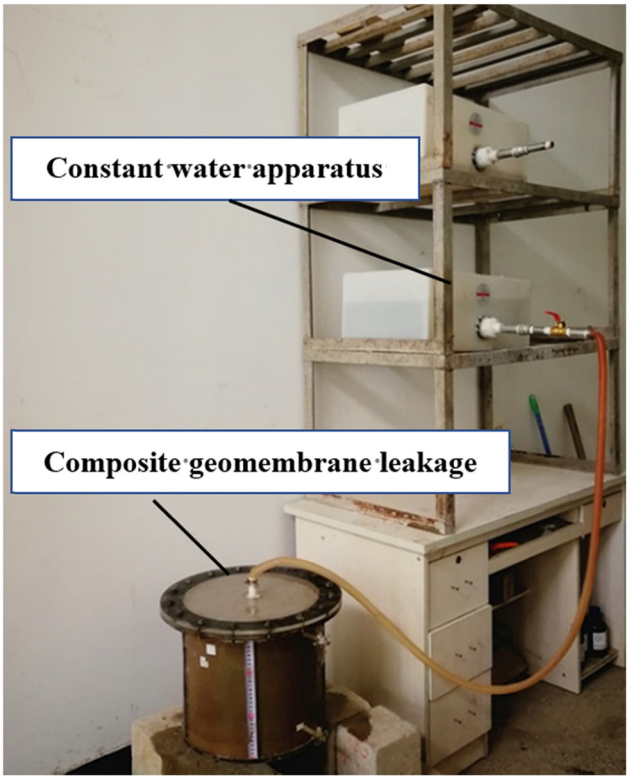

Figure 2: Realistic composite geomembrane leakage apparatus.

It can be seen from previous studies that many researchers have carried out laboratory tests or numerical simulation studies on the effects of composite geomembrane leakage (seepage size, water, and other factors) on earth-rock dams. However, these are more qualitative research and lacked specific quantitative analysis. Therefore, based on the Datun Reservoir of the ER-SNWTP (Eastern Route of the South-to-North Water Transfer Project), this paper combines laboratory tests and numerical simulation to discuss the quantitative influence of composite geomembrane leakage on Datun Reservoir. Firstly, the laboratory test of the influence of the leakage size and the water head on the leakage of composite geomembrane is designed. Secondly, laboratory tests, numerical calculation model, and Datun Reservoir numerical calculation model are established by using FLAC 3D (Fast Lagrangian Analysis of Continua in 3 Dimensions). Finally, the influence of leakage size, quantity, location (i.e., distance from dam toe), and water head of composite geomembrane is analyzed by orthogonal analysis and single-factor analysis.

2 Composite geomembrane defect leakage test

2.1 Testing apparatus

In this paper, a self-made composite geotextile defect leakage test apparatus is used. The test apparatus is shown in Figure 2. The main part of the test instrument is cylindrical. In the test apparatus, the upper permeable layer, composite geomembrane, cushion, soil, and the lower permeable layer are respectively filled from top to bottom (as shown in the filling soil samples module of Figure 3). The internal dimension of the composite geomembrane defect leakage test apparatus is 33 × 30 cm (diameter × height). The thickness of the upper permeable

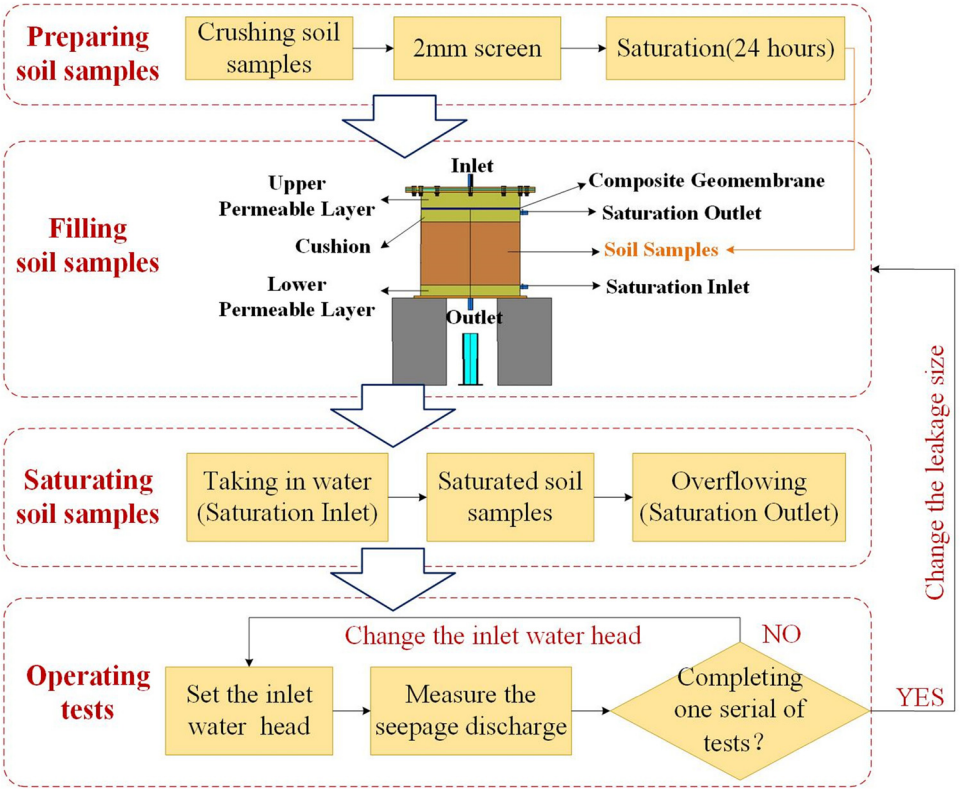

Figure 3: Testing procedure flowchart.

layer is 5 cm, which mainly prevents the flow from scouring the soil directly. To simulate the lower layer of geotextile film in practical engineering, the thickness of the cushion is 3 cm. The thickness of the soil sample is 20 cm, mainly to simulate the dam body of plain reservoir. The thickness of the sub permeable layer is 5 cm, mainly to prevent the loss of soil samples.

2.2 Testing materials

2.2.1 Soil

The test soil material is from the Datun Reservoir of ER-SNWTP. The size distribution curve of the soil sample is shown in Figure 4. The physical and mechanical parameters of soil samples are shown in Table 1. The compactness of soil samples in the test is consistent with the actual engineering, all of which is 97%.

2.2.2 Composite geomembrane

The structure of the composite geomembrane adopted in this paper consists of two layers and one membrane, as shown in Figure 5. The upper and lower sides are nonwoven cloth with a thickness of 1 mm, and the middle is 0.8 mm thick plastic film. The density of composite geomembrane used in the test is 550 g/m^2.

2.3 Testing scheme

The main factors affecting the leakage of composite geomembrane are the leakage size and the water head. Therefore, this paper designs an indoor test to analyze the influence of these two factors, as shown in Table 2.

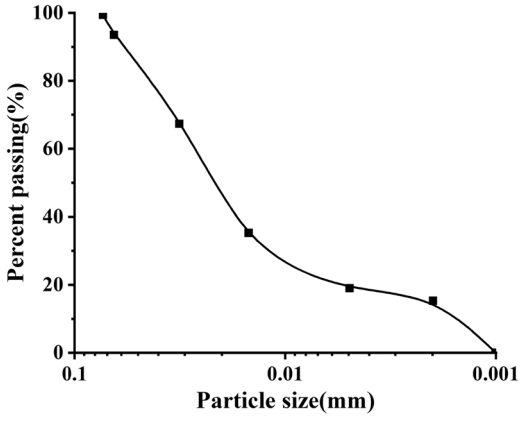

Figure 4: Particle size distribution curves of the tested soil.

Table 1: Material properties of the tested soil

Material	Clay content (<0.075 mm) (%)	Hydraulic conductivity (cm/s)	Liquid limit (%)	Plastic limit (%)	Specific gravity	Optimum moisture content (%)	Maximum dry density (g/cm^3)
Soil	19.8	7.67×10^{-5}	31.84	17.14	2.74	18.1	1.68

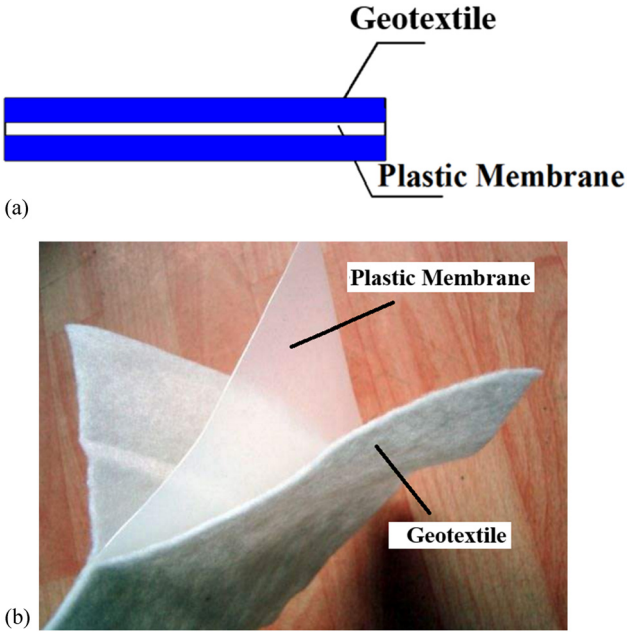

Figure 5: Composite geomembrane. (a) Schematic graph of composite geomembrane. (b) Realistic composite geomembrane.

Table 2: Testing schemes

Serial number	Leakage size (mm)	Water head (m)
T-1	2	1, 2, 3, 4, 5
T-2	5	1, 2, 3, 4, 5
T-3	10	1, 2, 3, 4, 5
T-4	20	1, 2, 3, 4, 5

2.4 Testing procedures

The test procedures are shown in Figure 3, which contain the following steps:

(1) Soil samples were first crushed and passed through a 2 mm screen. Optimum water content was maintained in the produced soil samples for 24 h, to ensure full water absorption.

(2) Secondly, 5 cm thick coarse sand is filled at the bottom of the composite geomembrane leakage test apparatus as the underlying layer. According to the test condition, the composite geomembrane is placed on the top of the soil sample by perforating the composite geomembrane. The glass glue was applied to the interface between the test apparatus and composite geomembrane to prevent water outflow from the interface. After the glass glue solidifies, fill the coarse sand as the upper layer. And close the top cover of the apparatus.

(3) Then water was fed from the saturated inlet, and once the water started to overflow out of the outlet (indication of full saturation), the tests were commenced. Increase the inlet head and adopt the measuring cylinder to measure the seepage discharge. After a serial of tests is completed, the leakage size can be changed to continue the test.

2.5 Testing results

The variation of seepage discharge with the water head under different leakage size is shown in Figure 6. It can be seen that the seepage discharge increases linearly with the water head. Furthermore, the seepage discharge increases as the levels of leakage size. This effect is found to be more obvious in the higher range of the leakage size. Only four leakage sizes (i.e., 2, 5, 10, and 20 mm) were investigated in the test. Therefore, the relationship between leakage size and seepage discharge will be investigated by numerical calculation.

3 Numerical calculation model of composite geomembrane leakage in Datun Reservoir

3.1 Numerical calculation model for laboratory tests

3.1.1 Composition of laboratory tests numerical calculation model

The three-dimensional numerical model of laboratory tests is established by FLAC 3D, as shown in Figure 7.

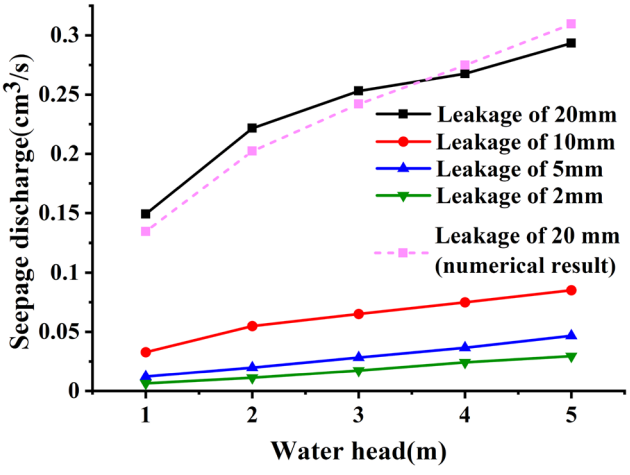

Figure 6: Testing results and numerical simulation verification result.

The dimensions of the numerical model are the same as the laboratory tests. The numerical model consists of 4,556 hexahedral elements and 1,891 nodes. The material parameters of soil in the numerical calculation model are shown in Table 1.

3.1.2 Boundary condition of laboratory tests numerical calculation model

In the numerical model of laboratory tests, both horizontal and vertical displacements are restricted at the side boundaries and vertical displacements are restricted at the bottom boundaries. Furthermore, the side boundaries are considered to be impermeable (i.e., no flow across the boundary); the value of pore water pressure at the top surface boundary is prescribed as zero and is not allowed to change throughout the analysis (i.e., $\Delta p = 0$); constant pore water pressure boundary conditions are employed at the bottom boundary to simulate the applied constant water head.

3.1.3 Simplified method of composite geomembrane of laboratory tests numerical calculation model

According to a large number of engineering investigations and analyses, Giroud found that geomembrane will produce one leakage every 4,000 m² in construction, and its equivalent aperture is generally in 1–20 mm [17]. The thickness of composite geomembrane is generally 0.2–3 mm, but the thickness is too small relative to the surrounding dam; it is difficult to have meshed when the model is built by FLAC 3D. Therefore, the principle of flow equivalence is adopted to select the appropriate thickness of the equivalent geomembrane to realize the modeling of composite geomembrane. The principle of flow equivalence is shown in equation (1).

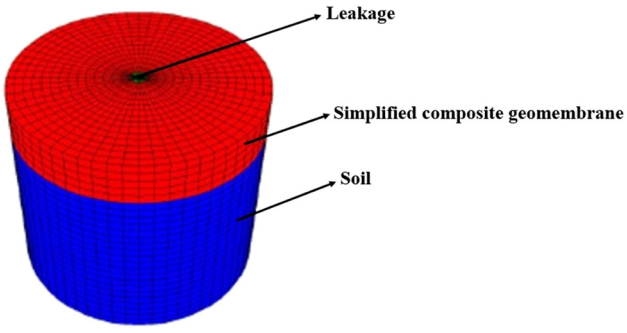

Figure 7: Numerical calculation model for laboratory tests.

$$Q_1 = \frac{\Delta h}{L_1} k_1 = \frac{\Delta h}{L_2} k_2 = Q_2 \tag{1}$$

where the Q_1, L_1, and k_1 are the seepage discharge, length of seepage paths, and hydraulic conductivity of composite geomembrane, respectively, the Q_2, L_2, and k_2 are the seepage discharge, length of seepage paths, and hydraulic conductivity of simplified composite geomembrane, respectively. According to the principle of flow equivalence, the thickness of composite geomembrane is converted into an equivalent soil layer with a thickness of 5 cm and a permeability coefficient of 1×10^{-11} cm/s.

3.2 Numerical calculation model for Datun Reservoir

3.2.1 Introduction of Datun Reservoir

The Datun Reservoir (shown in Figure 8) was selected as the research object, which is a typical plain reservoir with composite geomembrane. The designed water level in the reservoir is 10 m, the storage capacity is 52.09 million m^3, the height of the dam is 12.1 m, the width of the dam crest is 7.5 m, the slope ratio of the upstream slope is 1:2.75, and the slope ratio of the downstream slope is 1:2.5. The abandoned platform is below 7.4 m high. The width of the platform is 20 m, and the dam is filled with low liquid limit clay.

3.2.2 Composition of Datun Reservoir numerical calculation model

The three-dimensional numerical model of Datun Reservoir is established by FLAC 3D, as shown in Figure 9. The dimensions of the numerical model are the same as the Datun Reservoir. The width of the numerical model is 50 m. The

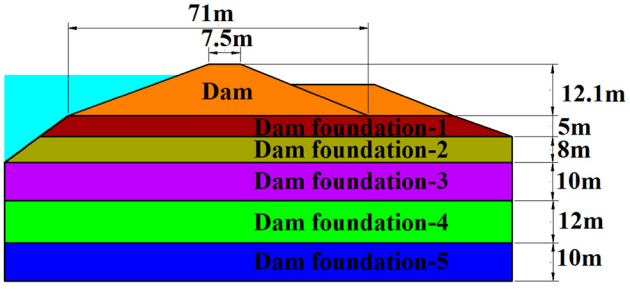

Figure 8: Datun Reservoir.

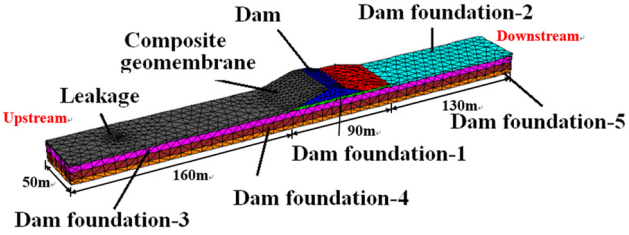

Figure 9: Datun Reservoir numerical model.

length of the dam foundation is 400 m. According to the actual situation, the dam foundation is divided into five layers. This model consists of 9,740 hexahedral elements and 2,305 nodes. The material parameters of the dam, dam foundation, and seepage control area in the numerical model are shown in Table 3. The upper surface of the composite geomembrane is the inlet surface, and the upper surface of the downstream slope of the abandoned platform and the dam foundation behind is set as a free drainage surface.

3.2.3 Boundary condition of Datun Reservoir numerical model

In the numerical model of Datun Reservoir, both horizontal and vertical displacements are restricted at the side boundaries and the bottom boundaries. Furthermore, the side boundaries are considered to be impermeable; the value of pore water pressure at the dam slope of the downstream and the top surface of downstream dam foundation is prescribed as zero and is not allowed to change throughout the analysis (i.e., $\Delta p = 0$); constant pore water pressure boundary conditions are employed at the top boundary of upstream dam foundation; gradient pore water pressure boundary conditions are employed at the dam slope of the upstream.

3.2.4 Simplified method of composite geomembrane of Datun Reservoir numerical model

It is noted that some simplified methods of composite geomembrane used in the laboratory tests calculation model were adopted in the Datun Reservoir numerical calculation model. The thickness of the composite geomembrane is converted into an equivalent soil layer with a thickness of 3 m and a permeability coefficient of 6×10^{-7} cm/s, and the leakage is converted into an

Table 3: Material parameters of numerical model

	Dam	Dam foundation-1	Dam foundation-2	Dam foundation-3	Dam foundation-4	Dam foundation-5
Bulk modulus (Pa)	8.60×10^6	9.55×10^6	1.66×10^7	1.17×10^7	5.89×10^7	5.63×10^7
Shear modulus (Pa)	7.40×10^6	4.13×10^6	3.82×10^6	2.89×10^6	8.91×10^6	8.91×10^6
Cohesion (Pa)	2.6×10^4	1.7×10^4	1.9×10^4	2.5×10^4	5.5×10^3	2.1×10^4
Angle of shearing resistance (°)	24.3	24	16.8	18.8	26.7	20.4
Dry density (g/cm^3)	1.93	1.95	1.96	1.98	1.94	2.03
Hydraulic conductivity (cm/s)	7.67×10^{-5}	5.37×10^{-4}	4.79×10^{-3}	3.07×10^{-4}	5.19×10^{-3}	4.05×10^{-4}

equivalent soil layer with a thickness of 3 m and permeability coefficient of 6×10^{-1} cm/s.

3.2.5 Numerical calculation schemes

Orthogonal analysis is carried out to analyze the sensitivity of seepage discharge of composite geomembranes leakage subjected to three critical soil properties (water level, leakage diameter, and distance from dam toe). Regardless of the interaction of the factors, the orthogonal table L9 (3^4) is used. The designed table of the influence factor level and the Orthogonal analysis are shown in Tables 4 and 5, respectively.

Based on the orthogonal analysis, the single-factor tests are also carried out to investigate the influence of the three factors on seepage discharge in detail. The designed testing scheme of the single-factor tests is shown in Table 6.

4 Numerical results and analysis

4.1 Numerical model verification

The numerical simulation and the experimental results are shown in Figure 6. The lack of matching between the experimental and simulated results is less than 10%. The simulation method of composite geomembrane leakage and the setting of water head application mode are accurate.

4.2 Orthogonal test results

The results from the orthogonal analysis are analyzed and discussed in this section. It is noted that the error analysis, range analysis, and variance analysis are carried out to analyze the effects of three critical soil properties.

Table 4: Level of influence factors

Level	Factors		
	A Water level (m)	B Leakage size (mm)	C Distance from dam toe (m)
1	3	2	10
2	5	10	50
3	10	20	150

Table 5: Testing scheme of orthogonal analysis

Test number	Factors		
	A Water level (m)	B Leakage size (mm)	C Distance from dam toe (m)
I-1	3	2	150
I-2	3	10	50
I-3	3	20	10
I-4	5	2	50
I-5	5	10	10
I-6	5	20	150
I-7	10	2	10
I-8	10	10	150
I-9	10	20	50

Table 6: Testing scheme of single-factor analysis

Tests number	Leakage size (mm)	Distance from dam toe (m)	Water head (m)	Leakage quantity	Gap between leakage (m)
II-1	2	100	10	1	0
II-2	5	100	10	1	0
II-3	10	100	10	1	0
II-4	20	100	10	1	0
II-5	30	100	10	1	0
II-6	2	100	1	1	0
II-7	2	100	3	1	0
II-8	2	100	5	1	0
II-9	2	100	7	1	0
II-10	2	100	10	1	0
II-11	2	10	10	1	0
II-12	2	50	10	1	0
II-13	2	100	10	1	0
II-14	2	130	10	1	0
II-15	2	150	10	1	0
II-16	20	100	10	2	10
II-17	20	100	10	3	10
II-18	20	100	10	4	10
II-19	20	100	10	3	0
II-20	20	100	10	3	5
II-21	20	100	10	3	15

4.2.1 Error analysis

The seepage discharge of orthogonal test results is shown in Table 7. SSj is the sum squares of each factor and SSE is the error sum squares. In the orthogonal test, the average seepage discharge is 64.44. The sum square of the water head is 1.40. The sum square of the leakage size is 0.82. The sum square of the distance from dam toe is 1.65. The error sum square of the orthogonal test is 0.04. The error sum square of the orthogonal experiment is much smaller than the sum squares of the factors. Therefore, the degree of the influence of error in the orthogonal experiment can be neglected.

Table 7: Critical hydraulic gradient of orthogonal test results

	A Water head (m)	B Leakage size (mm)	C Distance from dam toe (m)	E Empty column	Seepage discharge (m^3/day/50 m)
I-1	1 (3)	1 (2)	3 (150)	1	63.13
I-2	1 (3)	2 (10)	2 (50)	2	63.93
I-3	1 (3)	3 (20)	1 (10)	3	64.62
I-4	2 (5)	1 (2)	2 (50)	3	64.50
I-5	2 (5)	2 (10)	1 (10)	1	64.86
I-6	2 (5)	3 (20)	3 (150)	2	64.48
I-7	3 (10)	1 (2)	1 (10)	2	65.01
I-8	3 (10)	2 (10)	3 (150)	3	63.91
I-9	3 (10)	3 (20)	2 (50)	1	65.49
SSj	1.40	0.82	1.65	0.04	

4.2.2 Range analysis

The range analysis results are shown in Table 8. K_1, K_2, and K_3 in the table are the average values of seepage discharge under the same numerical condition of different factors. The results from the range analysis show that $R_C = 0.99 > R_A = 0.91 > R_B = 0.65$. R_A, R_B, and R_C are the range of degree of water head, leakage size, and distance from dam toe, respectively. This demonstrates that the distance from dam toe most has the greatest influence on seepage discharge. The influence of the water head is relatively less profound, while the leakage size shows the least impact.

4.2.3 Variance analysis

The data of the variance analysis of orthogonal test results are shown in Table 9. F test is used in variance analysis. It can be seen from the F value table that the value of $F_{0.025}(2,2)$ is 39 and that of $F_{0.05}(2,2)$ is 19. The variance analysis results of the orthogonal analysis show that the F of distance from dam toe is 42.58, which is greater than the value of $F_{0.025}(2,2)$, and its effect on the seepage discharge is highly significant. The F of water head and leakage size is 36.00 and 21.07, respectively, which is greater than $F_{0.05}(2,2)$, and its effect on the seepage discharge is significant. This is also in agreement with the results from the variance analysis. In particular,

Table 8: Range analysis results of interface internal erosion

	A Water head (m)	B Leakage size (mm)	C Distance from dam toe (m)
K_1	63.89	64.21	64.83
K_2	64.61	64.23	64.64
K_3	64.80	64.86	63.84
Range R_i	0.91	0.65	0.99

the results from the variance analysis show that the significance level of distance from dam toe is the highest, followed by water head and leakage size. Therefore, the impact order of the three factors is as follows: distance from dam toe > water head > leakage size.

4.3 Single-factor tests results

4.3.1 Leakage size

It is noted that the seepage discharge of 50 m in the simulated dam is 63 m³/d under the condition of no leakage. The leakage of composite geomembrane is located at the base of the dam 100 m away from the dam toe. The curve of the seepage discharge with the leakage size is shown in Figure 10(a). The leakage size increases from 0 to 5 mm, and the seepage discharge increases by 5.07%. The curve of leakage size and seepage discharge was fitted (i.e., the red solid line in Figure 10(a)). The results show that the seepage discharge of plain reservoir increases linearly with the increase of leakage size of composite geomembrane. The R-square of curve fitting is 0.99, which illustrates the curve fitting is accurate.

4.3.2 Water head

The leakage size of composite geomembrane is 2 mm, and the seepage discharge under different water head is shown in Figure 10(b). It can be seen that with the increase of the water head, the seepage discharge of the dam shows a linear increasing trend.

4.3.3 Distance from dam toe

The relationship between the seepage discharge and the distance from dam toe is shown in Figure 11. It can be seen that when the leakage location is less than 100 m away from the dam toe, the average seepage discharge is 65.00 m^3/day/50 m. However, when the distance from the dam toe exceeds 100 m, the seepage discharge decreases rapidly to 63.79 m^3/day/50 m with the increase of the distance from the dam toe. It shows that there exists a threshold distance; when the threshold is exceeded, the effect of leakage will suddenly decrease. The threshold distance is found to be 100 m, for the investigated cases.

4.3.4 Leakage quantity and distribution

The distribution of leakage points in the model is listed in Figure 12. Additional leakage point positions can be

Table 9: Variance analysis results of interface internal erosion

	A Water head (m)	B Leakage size (cm)	C Distance from dam toe (m)	E Empty column
K_{1j}^2	36735.86	37107.47	37823.25	37433.74
K_{2j}^2	37574.33	37133.29	37604.97	37407.43
K_{3j}^2	37795.64	37863.32	36678.38	37260.58
Free degree	2	2	2	2
SS	1.40	0.82	1.65	0.04
MS	0.70	0.41	0.83	0.019
F	36.00	21.07	42.58	
$F_{0.01}(2,2)$	99	99	99	
$F_{0.025}(2,2)$	39	39	39	
$F_{0.05}(2,2)$	19	19	19	
$F_{0.10}(2,2)$	9	9	9	
$F_{0.25}(2,2)$	3	3	3	
Significance level	* (Significant)	* (Significant)	** (Greatly significant)	

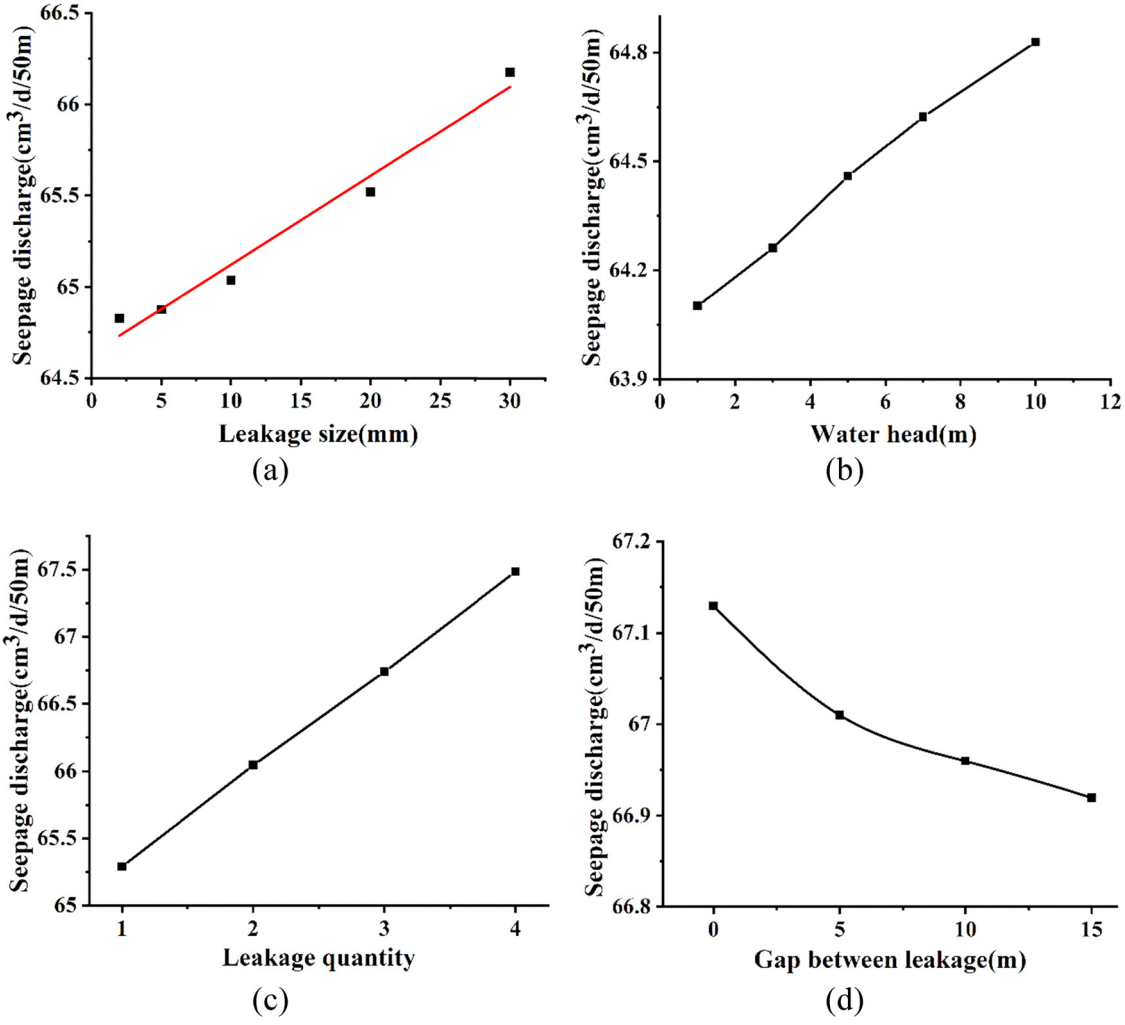

Figure 10: Seepage discharge for different impact factors (a) leakage size; (b) water head; (c) leakage quantity; (d) gap between leakage.

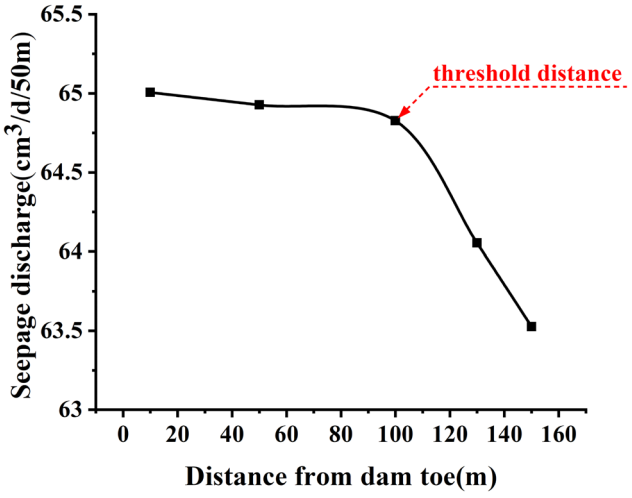

Figure 11: Seepage discharge for different distance from dam toe.

determined according to the basic leakage point and the leakage gap. The relationship between the seepage discharge and the leakage quantity is shown in Figure 10(c). It can be seen that the seepage discharge of the dam increases linearly with the increase of the leakage quantity. Figure 10(d) plots the distribution of leakage points and the variations of seepage discharge against the gap between leakage. It can be seen that with the increase of the gap, the seepage discharge decreases obviously. This effect is found to be more obvious in the higher range of the gap between leakage.

5 Innovation and limitation

The existed researches [12–16] about leakage of composite geomembrane are not enough to meet the need for an

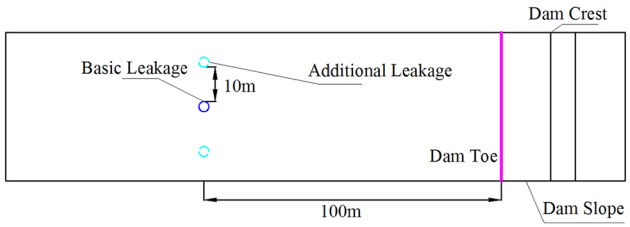

Figure 12: Distribution of leakage points.

increasing number of plain reservoirs which are effective methods to alleviate water scarcity in plains. Previous scholars [17–22] qualitatively researched several factors impacting the leakage of composite geomembrane, while the accurate and quantitative study about the sensitivity of various factors is lacking.

One innovation of this paper is comprehensively studying the influence of different factors on geomembrane leakage. The influencing abilities of various factors were analyzed and ranked (the distance from dam toe > water head > the leakage size). It is shown in the results that the leakage size, studied with great emphasis by most previous researchers, has the least impact on the leakage, compared with the distance from dam toe and the water head. The findings of this study have enlightening significance for future scholars to research in this field.

Besides, quantitative research of these factors was carried out, which was lacked in previous studies. A threshold distance is innovatively presented based on the quantitative analysis of the numerical results. The threshold distance is 100 m in the case study of Datun Reservoir. It indicates that the leakage of composite geomembrane should be paid attention to when the distance from the dam toe is less than 100 m. The results of this study have reference significance for the management, operation, and maintenance of similar projects.

It is true that the leakage shape of composite geomembrane is not always regular; most of the time it is shaped in slit or irregular curve, which can become a hot issue in future research. The numerical model built in this paper is an ideal model that may not simulate the practical situation accurately, but is suitable and enough to investigate the influencing ability of these factors quantitatively.

6 Summary and conclusion

In this paper, a self-made apparatus was applied to identify the influence of leakage size and water head on leakage of composite geomembrane. Furthermore, the numerical model of composite geomembrane leakage in the plain reservoir is established by FLAC 3D. The influence of three factors (i.e., the leakage size, water head, and distance from dam toe) on the seepage discharge of plain reservoir is analyzed by orthogonal and single-factor analysis. Combined with the numerical results, the following conclusions can be drawn:

(1) The difference between the results of laboratory tests and numerical model is less than 10%. It shows that the method of simplifying composite geomembrane by using the principle of flow equivalence is feasible.
(2) The impact order of the three factors on the seepage discharge of plain reservoir is the distance from dam toe > water head > leakage size. The seepage discharge increases as the water head, leakage size, and leakage quantity increase, in a linear relation. However, there exists a threshold distance; when the threshold is exceeded, the effect of leakage will suddenly decrease. The threshold distance is found to be 100 m, for the investigated cases.
(3) The numerical results showed that the leakage of composite geomembrane within the distance from the dam toe 100 m in the case study of Datun Reservoir should be paid attention to.

Acknowledgments: The authors appreciate the support of National Science and Technology Support Program (Grant No. 2015BAB07B05) and National Natural Science Foundation of China (Grant No. 41172267).

Conflict of interest: Authors state no conflict of interest.

References

[1] Ma JD. Study on feasibility of increase of water-storage depth for plain reservoirs. J Hohai Univ (Nat Sci). 2002;30(4):82–4.
[2] Han B, Geng F, Dai S, Gan G, Liu S, Yao L. Statistically optimized back propagation neural network model and its application for deformation monitoring and prediction of concrete face rockfill dams. J Perform Constr Facil. 2020;34(4):04020071.
[3] Muraleetharan KK, Liu C, Wei C, Kibbey TCG, Chen L. An elastoplatic framework for coupling hydraulic and mechanical behavior of unsaturated soils. Int J Plast. 2009;25(3):473–90.
[4] Zhang K, Liu SH, Wang LJ, Sun L, Fu YC. Numerical simulation of air field under geo-membrane in anti-seepage plain reservoir. South North Water Transf Water Sci Technol. 2012;10(5):97–100+118.
[5] Cheng WC, Ni JC, Huang HW, Shen JS. The use of tunnelling parameters and spoil characteristics to assess soil types:

a case study from alluvial deposits at a pipejacking project site. Bull Eng Geol Environ. 2019;78(4):2933–42.
[6] Cheng WC, Li G, Ong DEL, Chen SL, Ni JC. Modelling liner forces response to very close-proximity tunnelling in soft alluvial deposits. Tunn Undergr Space Technol. 2020;103:103455.
[7] Cheng WC, Wang L, Xue ZF, Ni JC, Rahman MM, Arulrajah A. Lubrication performance of pipejacking in soft alluvial deposits. Tunn Undergr Space Technol. 2019;91:102991.
[8] Sheil BB, Suryasentana SK, Cheng WC. Assessment of anomaly detection methods applied to microtunneling. J Geotech Geoenviron Eng. 2020;146(9):04020094.
[9] Peng TR, Wang CH. Identification of sources and causes of leakage on a zoned earth dam in northern Taiwan: hydrological and isotopic evidence. Appl Geochem. 2008;23(8):2438–51.
[10] Zhao MJ, Rong XU, Wang JJ, Wang P. Application of electrical resistivity tomography to leakage diagnosis of Earth rock-fill dam. J Chongqing Jiaotong University (Nat Sci). 2009;28(6):1097–101.
[11] Cheng WC, Li G, Liu N, Xu J, Horpibulsuk S. Recent massive incidents for subway construction in soft alluvial deposits of Taiwan: a review. Tunn Undergr Space Technol. 2020;96:103178.
[12] Cheng WC, Ni JC, Arulrajah A, Huang HW. A simple approach for characterising tunnel bore conditions based upon pipejacking data. Tunn Undergr Space Technol. 2018;71:494–504.
[13] Ai YM, Yin WD, Wang JX, Zhang LH. Application of plastic film and composite geo-membrane in seepage control of plain reservoir. J Water Resour Archit Eng. 2001;7(1):21–3.
[14] Zhou GH, Li WZ. Application of geosynthetics in plain reservoir construction. Water Sci Eng Technol. 1999;3:30–1.
[15] Liu ZQ, Gong Y, Kong XF, Zhao W, Liu F. Effect of calculation scope of dam foundation on seepage features of plain reservoir structures. Yellow River. 2015;37(12):106–10.
[16] Li CQ, Li CC, Wang S, Wang J. Anti-seepage performance of geomembrane used in plain reservoir. J Yangtze River Sci Res Inst. 2016;33(4):135–9.
[17] Shen ZZ, Jiang H, Shen CS. Numerical simulation of composite geomembrane defect leakage experiment based on saturated-unsaturated seepage theory. J Hydraul Eng. 2009;40(9):1091–5.
[18] Gan L, Shen ZZ, Yan ZQ, Ren HC. Numerical simulation of geomembrane defect leakage by saturated-unsaturated seepage method. Adv Mater Res. 2014;904:474–8.
[19] Peng YF, Hao D. Seepage characteristics analysis of geomembrane earthrock dams. Adv Mater Res. 2013;739:278–82.
[20] Barroso M, Touze N. Laboratory investigation of flow rate through composite liners consisting of a geomembrane, a gcl and a soil liner. Geotext Geomembr. 2006;24(3):139–55.
[21] Bouazza A, Vangpaisal T, Abuel-Naga H, Kodikara J. Analytical modelling of gas leakage rate through a geosynthetic clay liner–geomembrane composite liner due to a circular defect in the geomembrane. Geotext Geomembr. 2008;26(2):122–9.
[22] Ling C, Revil A, Abdulsamad F, Qi Y, Soueid Ahmed A, Shi P, et al. Leakage detection of water reservoirs using a Mise-à-la-Masse approach. J Hydrol. 2019;572:51–65.
[23] Peyras L, Royet P, Deroo L, Albert R, Becue JP, Aigouy S, et al. French recommendations for limit-state analytical review of gravity dam stability. Eur J Environ Civ Eng. 2008;12(9–10):1137–64.
[24] Holst BD. Numerical simulation of the flow in the interface of a composite bottom liner. Geotext Geomembr. 2005;23(6):513–33.
[25] Yang P, Ke J, Wang JG, Chow YK, Zhu F. Numerical simulation of frost heave with coupled water freezing, temperature and stress fields in tunnel excavation. Comput Geotech. 2006;33(6–7):330–40.
[26] Giroud JP, Badu-Tweneboah K, Bonaparte R. Rate of leakage through a composite liner due to geomembrane defects. Geotext Geomembr. 1992;11(1):1–28.
[27] Wu DZ, Yu L. Experimental study on the influence of defects in geomembrane on the seepage of a dam. J Zhejiang Sci-Tech Univ (Nat Sci Ed). 2016;35(3):474–8.
[28] Liu FR, Shen HJ, Wang TQ. Observation of leakage due to defects in geomembranes. South North Water Transf Water Sci Technol. 2004;2(2):49–51.
[29] Li X. The anti-seepage experimental study on a evaporation pond in inner Mongolia KeShenKeTengQi. Beijing: China University Geoscience; 2013.
[30] Sun D, Shen ZZ, Cui JJ. Seepage numerical simulation of geomembrane gravel dam caused by geomembrane defect. Water Resour Power. 2013;31(4):69–73.
[31] Cen WJ, Du XH, He HN. Seepage properties of geomembrane faced earth-rock dams under random multiple defects. Adv Sci Technol Water Resour. 2018;38(3):60–5.